

QUANTITATIVE X-RAY INSPECTION

F. Retraint – J.M. Dinten – R. Campagnolo
LETI (CEA – Technologies Avancées)
DSYS – CEA Grenoble
F-38054 Grenoble Cedex 09 – France

F. Peyrin
CREATIS / ESRF
INSA 502
69621 Villeurbanne Cedex– France

INTRODUCTION

In a radiograph the value of each pixel is related to the material thickness crossed by the X-Rays. Using this relationship, a defect in an object can be located and furthermore characterized by parameters such as depth, surface and volume.

Assuming a locally linear detector response and using a radiograph of reference object, the quantitative thickness map of the object can be obtained by applying offset and gain corrections [1]. However, for an acquisition system composed of a cooled CCD camera optically coupled to a scintillator screen, the radiographic image formation process generates some bias which prevent from obtaining the quantitative information : non uniformity of the X-Ray source, beam hardening, Compton scattering, scintillator screen and optical system responses ...

In a previous paper we had presented a model of scatter and beam hardening [1]. Here, in a first section, we propose a complete model of the radiographic image formation process taking account of these bias. In a second section, we present an inversion scheme of this model for a single material object which enables to obtain the thickness map of the object crossed by the X-Rays. By subtracting this map from the corresponding theoretical one, the quantitative map of the defects thickness is obtained.

In the third section, we describe an algorithm for the 3D reconstruction of the defects from a limited number of radiographs. This algorithm converges rapidly and provides an accurate description of defects geometry.

The process has been developed and tested for a quantitative X-Ray inspection of fuel rod welds.

CONTEXT OF THE STUDY

The object to inspect is a fuel rod with a sensitive part : the circular weld (see Figure 1.a). The acquisition system is composed of a cooled CCD camera optically coupled to a scintillator screen (see Figure 1.b). Assuming a locally linear detector response, the model of the radiographic image formation is given by the following equation :

$$\phi(s) = \rho\phi_0 e^{-\mu.l(s)} \quad (1)$$

where s is the site on the detector, ϕ_0 is the incident flux, μ is the attenuation coefficient, $l(s)$ is the material thickness crossed by the X-rays at site s and ρ is the conversion coefficient.

RADIOGRAPHIC IMAGE FORMATION

The successive phenomena which occur in the image formation process are described from the X-Rays generation (X-Ray source) to the detector (CCD camera), in the following of this paper. These phenomena modify the equation (1).

X-Ray Source

- The non punctual X-ray source generates a blurring on the detector. This phenomenon is modeled by a convolution kernel depending on the distance between the X-Ray source and the detector, the distance between the object and the detector, and the size of the focal spot(see Figure 2.a).
- The X-ray source generates a non uniform photon flux (see Figure 2.b) which leads to an incident flux depending on the site s , $\phi_0(s)$. This phenomenon is measured by an acquisition without object.

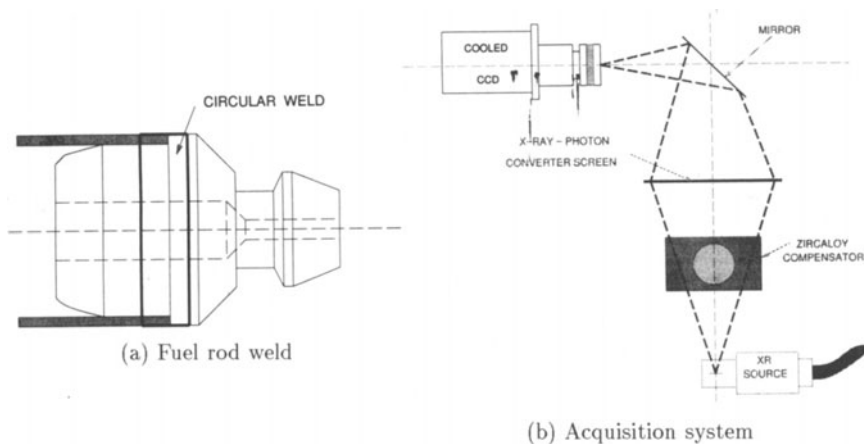


Figure 1. Context of the study.

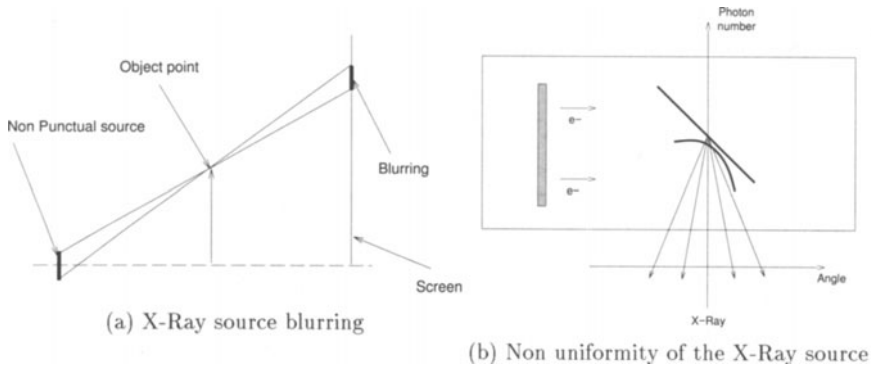


Figure 2. X-Ray source.

Incoherent Scattering

This phenomenon generates a scattered photon flux, S_{object} , which is added to the non attenuated flux, ϕ_{direct} . The incoherent scattering is characterized by two factors : the Compton attenuation coefficient which models the occurrence probability of the incoherent interaction and the Klein et Nishina law describing the scattering direction. Either, this scatter distribution is experimentally estimated by sampling its value with a grid stopping the direct flux, and fitting a low frequency surface through these samples values. Or, because of its low frequency shape, it is often estimated by a low pas filter of acquired radiograph [3]. Our approach of scatter evaluation and correction is based on a physical model of its formation process.

In the context of the application presented in this paper, the scatter distribution can be expressed by a functional of the direct flux :

$$S_{object} = \mathcal{F}(\phi_{direct}) = \mathcal{F}(\phi_0 \cdot e^{-\mu \cdot l}) \quad (2)$$

Beam Hardening

The physical coefficients characterizing the interaction between X photons and the material vary according to the X-Ray energy. Figure 3.a shows the absorption coefficient variations of Zircalloy versus X-Ray energy. As it is shown on Figure 3.b, the X-Ray source spectrum presents a large energy band. In the case of the single density object considered in this paper, the beam hardening can be modeled by a mean attenuation coefficient which depends on the thickness crossed by the X-Rays, $l(s)$, at each site s . This mean coefficient is obtained by an adapted calibration.

Light Image Formation

The conversion process of X photons into light photons and the light image transmission in the optical system degrade the radiograph quality :

- As demonstrated by Swank [2], the X photons conversion into light photons generates a blurring (see Figure 4.a) characterized by a point-spread-function, H_{screen} , which depends on the absorption coefficient of the X photons in the

screen, on the light absorption and diffusion coefficients in the screen and on the screen thickness.

- The main phenomenon which occurs during the light image transmission in the optical system is aperture aberration [5] (see Figure 4.b). It is modeled by a convolution kernel, H_{optic} , depending on the light wavelength generated by the the screen, on the optical aperture diameter and on the distance between the optical system and the detector.

From an experimental point of view, the point-spread functions are determined by measuring the response of a slit across the scintillator screen and the optical system.

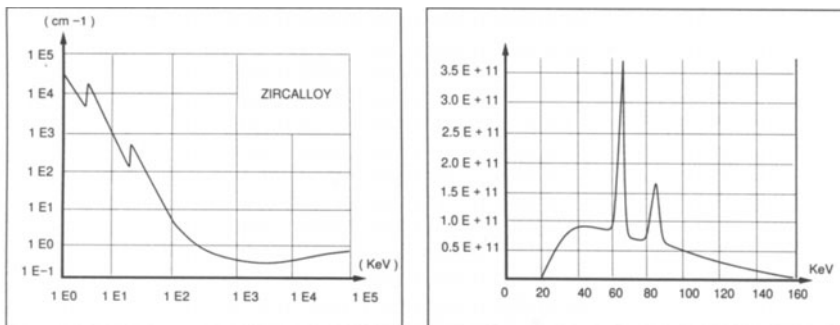
CCD Camera

- Each pixel of the CCD camera presents an offset. The offset map, I_n , is called "black image" and is obtained from an image without light.
- Each pixel has a different response gain. This gain is obtained by an acquisition without object.

Noise

The image formation process generates different sources of noise :

- the X photon flux is Poisson distributed,
- the process of conversion from X-Rays into light photons can be approached by a Poisson distribution,
- the light transmission across optical system is a "binary selection" process,
- the electron production process in the CCD detector is also a "binary selection" process.



(a) Absorption coefficient variations of zicalloy

(b) X-Ray source spectrum

Figure 3. Beam hardening.

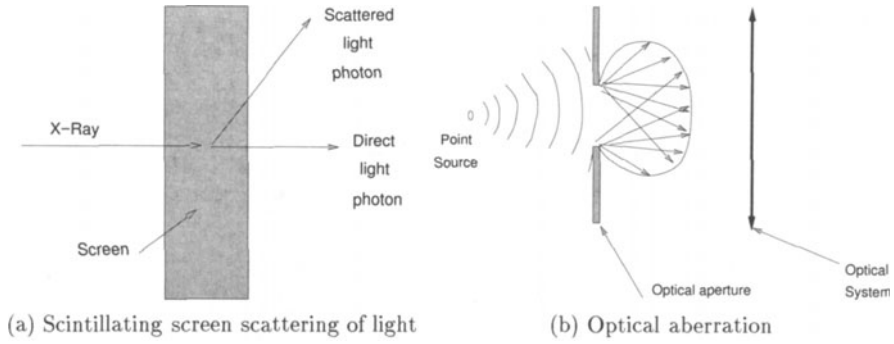


Figure 4. Light image formation.

A combination of these distributions leads to an estimation of the noise variance in the radiographs, $\widehat{\phi}_{CCD}$:

$$\sigma_{\phi_{CCD}}(s) = \sqrt{(1 + \rho)} \sqrt{\widehat{\phi}_{CCD}(s)} \quad (3)$$

Assuming an additive noise $N(s)$ of variance $\sigma_{\phi_{CCD}}(s)$, the final model of the radiographic image formation can be written :

$$\begin{aligned} \phi_{CCD}(s) = & \rho \cdot g(s) \cdot (\phi_0(s) \cdot e^{-\mu_{ph}(l(s)) \cdot l(s)} + S_{object}(s)) \\ & * H_{focalspot} * H_{screen} * H_{optic} + I_n(s) + N(s) \end{aligned} \quad (4)$$

INVERSION SCHEME OF THE MODEL

By resolving equation (4), the tickness map, $l(s)$, can be built from the acquired image $\phi_{CCD}(s)$. The global resolution is obtained by a sequence image processing treatments :

1. Subtraction of "black image", I_n ,
2. Correction of the pixels gain and the non uniformity of the X-Ray source. This correction is obtained by division by an image without object.
3. The deconvolution of the screen, optical and X-Ray source blurrings is realised with a Wiener filter adapted to the non uniformity of the noise.
4. Correction of the scatter distribution. This correction is obtained by the resolution of the following equation :

$$\phi_{Obs} = e^{-\mu \cdot l} + \mathcal{F}(e^{-\mu \cdot l}) \quad (5)$$

Where ϕ_{Obs} is image obtained after the step 3. To resolve this non linear problem, we apply a fixed point algorithm.

5. The beam hardening is evaluated by an adapted calibration.

These corrections lead to the mesure of thickness crossed by the X-Rays.

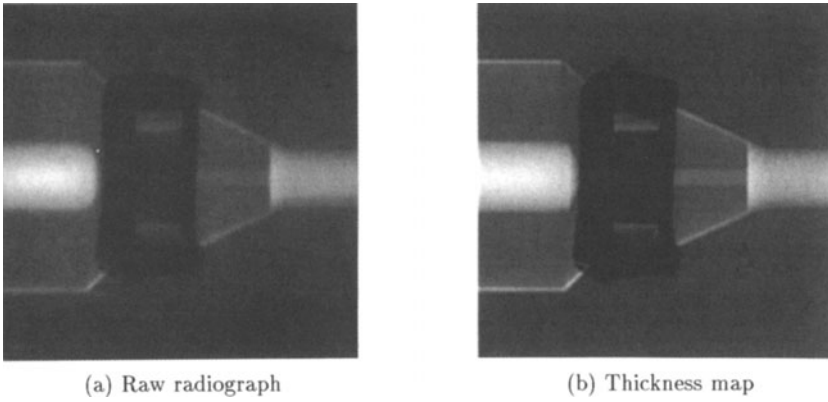


Figure 5. Light image formation.

RESULTS

The image of Figure 5.a shows the result obtained after the bias correction in the radiograph of fuel rod (image of the Figure 5.b). We can note a raising of the contrast in the image. The Figure 6 shows the theoretical thickness and the thickness crossed by X-Rays after the bias correction, in the circular weld zone of the fuel rod : it can be noted that the reconstruction thickness (continuous curve) fits perfectly with the one given by the CAD model (triangular marks).

CONSTRUCTION OF DEFECTS MAP

To obtain defects map, we realize a matching between a reference object thickness map and a thickness map of an object with defects (see Figure 7). The Figure 8 shows an example of defects thickness map.

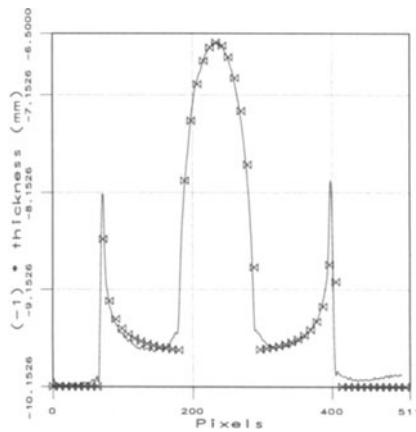


Figure 6. Thickness in circular weld zone.

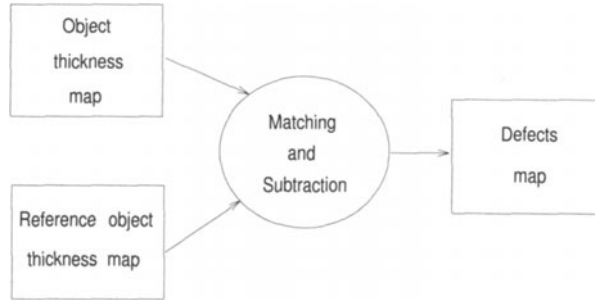


Figure 7. Construction of defects map.

DEFECTS RECONSTRUCTION

The 3D reconstruction problem is given by the following equation :

$$y = Hx + \epsilon$$

where H is the projection matrix of radiographs, y is the vector of defects map, ϵ is the vector of noise on the projection and x is the vector of defects.

The fuel rod welds inspection is realized from 3 equidistributed radiographs. Because of the noise in the defects map and the limited number of projections, the reconstruction problem is an ill-posed inverse problem. To obtain a solution, we introduce some a priori information in the resolution of inverse problem. We know that the defects in the fuel rod are a single density object and homogeneous. To introduce these a priori, we use a binary Markovian model, called Ising Model [6]. This model is defined by the following energy :

$$U(x) = \beta \sum_{(i,j)} 1_{x_i \neq x_j}$$

where (i, j) define the relation between the neighbor elements i et j of the vector x , x_i is the defect density at the site i and β is the cost of the configuration $x_i \neq x_j$.

$\beta \leq 0$ favors a texturized distribution, whereas $\beta \geq 0$ favors an homogeneous distribution, as the one presents in defects.

Assuming an additive Gaussian noise with a non stationary variance, the solution of the reconstruction problem is determined by the minimization of the following equation :

$$E(x) = \sum_r \frac{\|y_r - (Hx)_r\|^2}{\sigma_r^2} - \beta \sum_{(i,j)} 1_{x_i \neq x_j}$$

Where r is a projection site and σ_r^2 is the noise variance on this projection site.

The minimization is realised by a determinist algorithm, called ICM (Iterated Conditional Mode) [6]. This algorithm converges rapidly to a local minimum of the energy which depends on the initialization and on the scanning

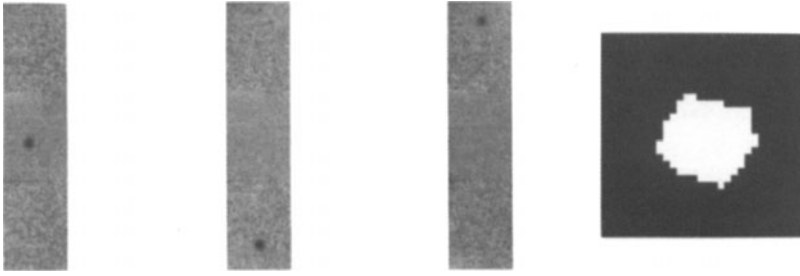


Figure 8. Example of defects reconstruction.

mode of the object sites. The reconstruction result of a defect from 3 maps is presented on the Figure 8.

CONCLUSION AND PERSPECTIVES

In this paper we have presented an efficient processing of radiographs which enables to build up a map of the materials thickness crossed by the X-Rays. This processing leads to a precise detection and characterization of defects. From a limited point of views, a Markovian regularized reconstruction algorithm provides a 3D description of defects. The presented process of thickness map reconstruction has now to be generalized to multi densities object if some a priori information are available. For the 3D reconstruction, the presented resolution algorithm is highly dependent on the initialization. We are working on the development of a new algorithm which is faster and leads to better reconstruction.

ACKNOWLEDGEMENTS

This work is supported by the Franco-Belge de Fabrication de Combustibles.

REFERENCES

1. F. Retraint, J.M. Dinten., "Beam hardening and scattering correction for a quantitative X-ray inspection of fuel rods", Review of Progress in Quantitative NDE, (1996).
2. R.K. Swank, "Calculation of Modulation Transfer Functions of X-ray fluorescent screens", Applied Optics vol. 12 No. 8, (1973).
3. F.C. Wagner and A. Mascovski, "A Characterization of Scatter Point-Spread-Function in Terms Of Air Gaps", Information systems laboratory, Stanford University, IEEE Trans. on Medical Imaging (1988).
4. C. Burq, "Modèles de dégradation en radiographie et restauration d'image", Ph.D. Thesis, Université Paris Sud (1992).
5. B. Peters, D. Meyer-Ebrecht, "System analysis of X-ray CCDs and adaptative restoration of intraoral radiographs", SPIE vol 2710, (1996).
6. J. Besag, "On the statistical analysis of dirty picture", A. Royal. Stat. Soc. Series B, B-48:259-302, (1986).